Pharmaceutical Biotechnology

Effect of Antimicrobial Preservatives on Partial Protein Unfolding and Aggregation

REGINA L. HUTCHINGS, SURINDER M. SINGH, JAVIER CABELLO-VILLEGAS, KRISHNA M.G. MALLELA

Department of Pharmaceutical Sciences & Center for Pharmaceutical Biotechnology, Skaggs School of Pharmacy and Pharmaceutical Sciences, University of Colorado Anschutz Medical Campus, 12850 E Montview Blvd, C238-V20, Aurora, Colorado 80045

ABSTRACT: One-third of protein formulations are multi-dose. These require antimicrobial preservatives (APs); however, some APs have been shown to cause protein aggregation. Our previous work on a model protein cytochrome *c* indicated that partial protein unfolding, rather than complete unfolding, triggers aggregation. Here, we examined the relative strength of five commonly used APs on such unfolding and aggregation, and explored whether stabilizing the aggregation 'hot-spot' reduces such aggregation. All APs induced protein aggregation in the order m-cresol > phenol > benzyl alcohol > phenoxyethanol > chlorobutanol. All these enhanced the partial protein unfolding that includes a local region which was predicted to be the aggregation 'hot-spot'. The extent of destabilization correlated with the extent of aggregation. Further, we show that stabilizing the 'hot-spot' reduces aggregation induced by all five APs. These results indicate that m-cresol causes the most protein aggregation, whereas chlorobutanol causes the least protein aggregation. The same protein region acts as the 'hot-spot' for aggregation induced by different APs, implying that developing strategies to prevent protein aggregation induced by one AP will also work for others. © 2012 Wiley Periodicals, Inc. and the American Pharmacists Association J Pharm Sci 102:365–376, 2013

Keywords: antimicrobial preservatives; protein formulations; protein aggregation; protein structure; stability; proteins; benzyl alcohol; phenol; m-cresol; phenoxyethanol; chlorobutanol; cytochrome *c*

INTRODUCTION

Protein-based pharmaceuticals comprise a significant portion of drug formulations. More than 350 parenteral formulations are available worldwide, with almost 150 protein-based pharmaceutical drugs commercially available in the United States.[1–2] One-third of these parenteral products are multidose,[3] which are advantageous in terms of patient compliance as well as economics. Protein formulations require a shelf-life stability of 18–24 months.[4] To maintain product viability, multidose formulations require the

presence of antimicrobial preservatives (APs)[3,5] to inhibit the growth of microbes and bacteria during repeated contact between the solution and a syringe needle.[3] APs are also found in topical ointments,[6] and in multidose delivery systems such as mini pumps for continuous infusion[7] and injection pens.[8]

The use of APs in protein formulations is of recent concern because of the discovery that these small molecules induce protein aggregation. In one of the first reports, Maa and Hsu[9] demonstrated that the addition of aromatic and aliphatic alcohols results in the aggregation of human growth hormone. Similar results were found with APs, most of which are alcohols, and with other proteins. For example, benzyl alcohol (BA), the most widely used AP, induces the aggregation of interferon-γ,[10] interleukin-1 receptor antagonist,[11] and human granulocyte colony-stimulating factor[12]; m-cresol (CR) induces the aggregation of human growth hormone[9,13] and interleukin-1 receptor[14]; and phenol (PH) induces the aggregation of an antibody.[15] Such protein aggregates in formulations can decrease the efficacy of the
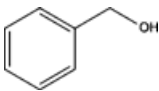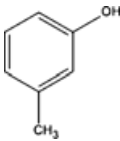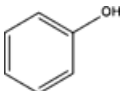

Table 1.   Antimicrobial Preservatives Used in this Study

AP	Molecular Structure	Molecular Weight (Da)	Source	Purity (%)
Benzyl alcohol (BA)		108.1	Merck	97
4-Chloro-1-butanol (CB)		108.6	Sigma	85
m-Cresol (CR)		108.1	Sigma	99
Phenol (PH)		94.1	Sigma	99.5
2-Phenoxyethanol (PE)		138.2	Fluka	99.5

delivered drug as well as stimulate undesirable toxic and immunologic responses in patients.[16–27] Therefore, an understanding of the molecular mechanisms underlying AP-induced protein aggregation and the development of strategies to minimize such aggregation are of paramount importance in developing stable multidose drug formulations.

Out of the eight commonly used APs,[3,5] five (listed in Table 1) are specifically used in liquid protein formulations. However, it has not been clear whether all five APs result in protein aggregation, and to what extent. Preliminary evidence from Maa and Hsu[9] indicates that various alcohols induce the aggregation of human growth hormone to different extents, implying that protein aggregation may depend on the nature of the alcohol. Such comparative information on APs is not available, which will be helpful in choosing the right AP when designing a stable therapeutic formulation so that the formation of protein aggregates and the resultant immunogenic and toxic effects can be minimized.

The ideal method of understanding aggregation mechanisms is to study how various APs induce the aggregation of a pharmaceutical protein of interest using biophysical methods. However, most pharmaceutical proteins are relatively less understood in terms of their biophysics and solution behavior. Therefore, we used a model protein, cytochrome c (Cyt c; Fig. 1), which has been well characterized in the literature. This protein offers many spectroscopic probes because of its covalently linked heme chromophore, in addition to the traditional signals such as circular dichroism and fluorescence of aromatic residues used to monitor protein structure. A

particularly useful tool to probe the partial unfolding of Cyt c is an absorption band at 695 nm that reports on the unfolding of one of the least stable regions in the protein (Red-colored Ω-loop in Fig. 1). In Cyt c, the methionine residue at position 80 (Met80) that is part of this Red loop is covalently linked to the ferric iron of the heme group. The 695 nm band originates due to charge transfer from the side-chain
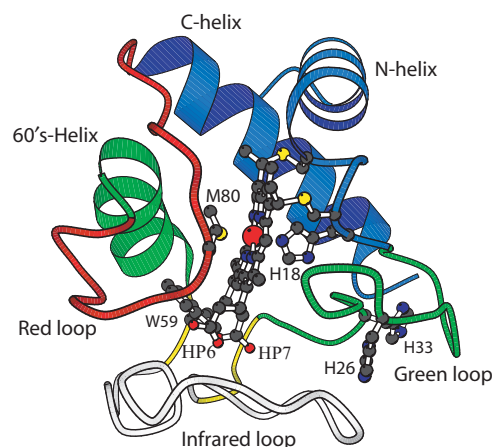
Figure 1. Molecular structure of cytochrome c (Cyt c; 1HRC.pdb). The protein consists of three α-helices and three Ω-loops. Individual cooperatively unfolding regions detected in Cyt c are colored in terms of their increasing stability: Infrared (Nested-yellow), Red, Yellow, Green, and Blue.[30] The unfolding of Cyt c proceeds either through the Red loop or through the bottom Infrared loop.[30] The figure also shows the covalently linked heme, and its two axial ligands His18 and Met80. The structure was generated using the MOLSCRIPT[38] program.

sulfur of Met80 to the ferric iron. When the local region around Met80 unfolds, this absorption band is absent because of the breakage of the Met80 to heme bond. The identification of the Ω-loop containing Met80 as being a least stable region, or weakest link in the protein, came from earlier residue-resolved hydrogen exchange (HX) experiments measured using two-dimensional nuclear magnetic resonance (2D NMR) spectroscopy,[28–31] protein unfolding monitored in response to various stresses,[32–34] and from studies on ultrafast protein dynamics.[35] Our earlier computational analysis predicts that the six residues around Met80 act as an aggregation "hot-spot" whose unfolding may lead to Cyt c aggregation,[36] and experimental results confirm this hypothesis.[36] Subsequent determination of the molecular structures of Cyt c oligomers using X-ray methods and their characterization using biophysical techniques[37] indicate that the aggregates have the same native structure as that of monomeric Cyt c with no change in the secondary structure (identical circular dichroism spectrum), except that the C-terminal helices are domain swapped between the monomers, and the Met80 region is unfolded. These earlier results on Cyt c, which determined the nature of partial protein unfolding that leads to aggregation, provide a unique opportunity to test the effect and relative strength of different APs on protein unfolding and aggregation. We have also tested whether stabilizing the local protein region that acts as the aggregation "hot-spot" will reduce the AP-induced protein aggregation.

MATERIALS AND METHODS

Materials

Equine Cyt c (Type VI) was obtained from the Sigma Chemical Company (St. Louis, Missouri). Before experiments, the protein was oxidized using potassium ferricyanide (Fisher Chemicals, Fair Lawn, New Jersey) to remove any trace amounts of the reduced form, dialyzed extensively against the desired buffer, and filtered through a 0.22 μm filter. The purity of the protein was determined from the ratio of the absorbance values at 409 nm (heme Soret band) and 280 nm (aromatic absorption band), which was 4.6 as expected for a pure oxidized protein.[39] In addition, the absence of the reduced form in the sample was confirmed from the absorbance values at 339, 526.5, 541.74, and 550 nm using a previously described method.[39–40] For experiments with the reduced form, sodium dithionite (Sigma Chemical Company) was used to reduce Cyt c.[41] The five APs used in this study are listed in Table 1.

Preservative Efficacy Test

To confirm the antimicrobial activity of APs, a simplified preservative efficacy test was performed.[42] A primary culture of *Escherichia coli* DH5α cells was incubated overnight at 37°C in a shaker. Aliquots of 0.5 mL were transferred into six 50 mL culture flasks containing either no preservative (control), or one of the five APs. Cultures were incubated at 37°C with shaking for 6 h, and optical density at 600 nm was used to measure the cell growth kinetics.

Size-Exclusion Chromatography

To monitor the effect of BA on protein aggregation, Cyt c (2 mM in 0.1 M sodium phosphate, 0.15 M sodium chloride, pH 7) was incubated at 37°C on a rotator (Thermo Scientific Labquake Shaker Rotisserie, West Palm Beach, Florida) and samples were taken at desired intervals. Concentration of the monomer was estimated by injecting 5 μL onto a TSKgel 5 μm G3000SWxl column (Tosoh Bioscience LLC, San Francisco, California) on an Agilent 1100 HPLC (Santa Clara, California). The mobile phase used for this column was 0.1 M sodium phosphate, 0.1 M sodium sulfate, pH 6.7 at a flow rate of 0.7 mL min⁻¹. Absorbance at 280 nm was used to estimate the protein concentration. The average of 0% (v/v) BA triplicates on day 0 was used to normalize the peak area of subsequent sample sets.

Isothermal Incubation Experiments

Cyt c solution was incubated at the desired temperature, and the changes in optical density at 695 and 800 nm were measured as a function of the incubation time. For these experiments, the cuvette of buffer solution was initially equilibrated at the desired temperature, and Cyt c (300 μM final concentration) was added to the cuvette. The aggregation kinetics was monitored until the signal reached a plateau. At longer incubation times, the aggregates started to settle down to the bottom of the cuvette, resulting in decreased optical density. At that point, the experiment was stopped.

Thermal Scanning Method

The aggregation temperature (T_m^{Agg}) of the protein was measured using a thermal scanning method on a Chirascan Plus spectrometer (Applied Photophysics, Surrey, UK). The temperature was increased at a rate of 1°C/step followed by 2 min equilibration, and changes in the optical density at 800 nm were recorded. T_m^{Agg} was determined using Global Analysis T-Ramp software (Pro-Data Global3 v1.1.0), provided by Applied Photophysics using a single transition and double baseline correction. For these

experiments, $300\,\mu\mathrm{m}$ Cyt c in $0.1\,\mathrm{mM}$ sodium phosphate, $0.15\,\mathrm{mM}$ sodium chloride, pH 7 was used. The reduced Cyt c samples contained sodium dithionite ten times that of protein concentration to maintain Cyt c in reduced form during thermal scanning.

Temperature unfolding of the Met80 region was performed by monitoring changes in the optical density at 695 nm using the above described thermal scanning method. The optical density initially decreased followed by an increase. From the initial decrease, the melting temperature (T_m^{695}) was determined as the temperature at which the absorbance is half of the difference between the absorbance values of the native and unfolded states. Absorbance of the unfolded state at high temperature was independently measured by denaturing $300\,\mu\mathrm{M}$ Cyt c with 6 M GdmCl.

Denaturant Melts

Guanidinium chloride (GdmCl) was used as the denaturant. Protein solutions at varying GdmCl concentrations were prepared and equilibrated overnight before measuring changes in optical signals as a function of the denaturant concentration. Concentration of the denaturant was determined using refractive index measurements.[43] For measuring changes in the 695 nm absorbance, $300\,\mu\mathrm{M}$ Cyt c in $0.1\,\mathrm{M}$ sodium phosphate, $0.15\,\mathrm{M}$ sodium chloride, pH 7 was used. The ΔG values were determined by fitting the changes in optical signals at different denaturant concentrations to a two-state unfolding model.[44–45]

Nuclear Magnetic Resonance

Two-dimensional homonuclear gradient COrrelation SpectroscopY (COSY) experiments were run to monitor changes in Cyt c amide cross-peaks as a function of the AP using a Varian Inova 600 MHz NMR instrument (Palo Alto, California) equipped with a cryoprobe. For these experiments, 3 mM Cyt c ($0.1\,\mathrm{M}$ sodium phosphate, $0.15\,\mathrm{M}$ sodium chloride, pH 7) and deuterated APs (0.8%, v/v) were used. Deuterated chlorobutanol (CB) was not available commercially, and hence the NMR experiments were performed with the other four deuterated APs (Isotec Inc., Miamisburg, Ohio). The NMR spectra were collected with 8000 Hz spectral width and 512 points in each direction. The spectra were processed in magnitude mode using the nmrPipe software (Frank Delaglio, National Institutes of Health) with zero filling to twice their real points, apodization with nonshifted sine multiplication, exponential broadening, and Gaussian transformation. The spectra were baseline corrected in both dimensions. Changes in the peak positions (chemical shifts) and peak volumes were calculated using the nmrDraw package (Frank Delaglio, National Institutes of Health). Cyt c

residue assignments available in the literature[46] were used for this purpose. 4,4-Dimethyl-4-silapentane-1-sulfonic acid was used as a standard to reference the chemical shifts as well as to normalize the measured changes in cross-peak volumes with the addition of APs.

Hydrogen Exchange

Cyt c (3 mM), whose amides were protons, was lyophilized in deionized water. It was dissolved in the appropriate buffer in D_2O just before running the HX experiment and filtered through $0.22\,\mu\mathrm{m}$ filter. A series of 2D gradient COSY spectra was recorded back to back using a Varian Inova 600 MHz NMR instrument equipped with a cryoprobe to monitor the HX of various amide hydrogens. NMR spectra were processed using nmrPipe software and the changes in peak volumes due to exchange were measured using nmrDraw software. The changes in peak volumes due to exchange were normalized with the intensities of five nonexchangeable cross-peaks.[36]

RESULTS

Antimicrobial Activity of APs

To demonstrate the antimicrobial efficacy of the five APs, we tested their effect on the growth of *E. coli* bacteria.[42] For this purpose, we used DH5α cells in LB media and monitored the cell count by measuring changes in the optical density at 600 nm as a function of the growth time. Without APs, the growth curve showed an exponential increase (Fig. 2). However, no increase in the optical density was observed with the addition of any of the five APs, indicating that these molecules inhibited bacterial growth.

APs Induce Cyt *c* Aggregation

Earlier studies have indicated that APs cause aggregation of pharmaceutical proteins over a course of several days and months when stored close to room temperature.[9–15] Monitoring the effect of different APs on such aggregation and at different solution conditions is not feasible because of long incubation times. Therefore, to probe the aggregation mechanisms on a convenient laboratory scale, we accelerated the aggregation kinetics by performing isothermal incubation studies at higher temperatures. We first showed that APs induce Cyt c aggregation at physiological temperatures by following the concentration of the Cyt c monomer in solution as a function of the incubation time, using BA as the AP (Fig. 3a). Over a time course of four days, 3% (v/v) BA aggregated Cyt c by 50%, whereas no such aggregation was observed in the absence of AP. We further examined the effect of temperature on the kinetics of
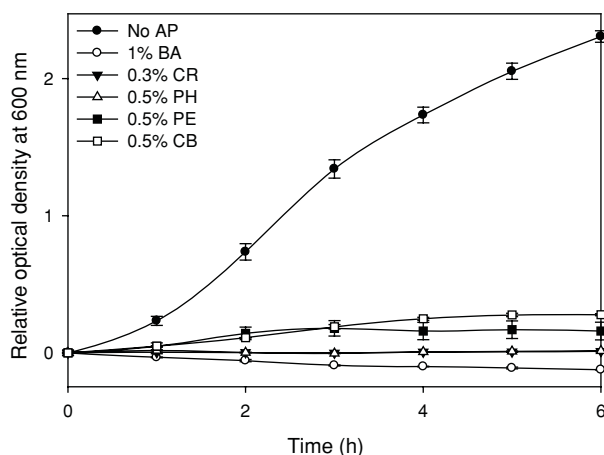
Figure 2. Preservative efficacy test of APs on DH5α *E. coli* cells.[42] The filled circles represent the data untreated with APs, whereas the other symbols represent the data treated with various APs: 1% (v/v) benzyl alcohol (BA), 0.3% (v/v) m-cresol (CR), 0.5% (v/v) phenol (PH), 0.5% (v/v) phenoxyethanol (PE), and 0.5% (v/v) chlorobutanol (CB). These concentrations correspond to those used in protein formulations. The cell count was monitored by measuring the relative optical density at 600 nm as a function of the growth time. Addition of APs inhibited bacterial growth.

AP-induced protein aggregation (Fig. 3b). With the increase in solution temperature from 65°C to 85°C, the rate of Cyt *c* aggregation induced by 0.8% (v/v) BA increased. On the basis of this data, we chose 75°C (Fig. 3c) and 80°C (Fig. 3d) so that the effect of APs on Cyt *c* aggregation can be conveniently monitored on the timescale of hours. The rate and extent of aggregation depends on the nature of AP. The five APs followed the order CR > PH > phenoxyethanol (PE) > BA > CB. Under identical conditions, no aggregation was observed for Cyt *c* in the absence of APs. For these comparison experiments, a concentration of 0.8% (v/v) was chosen for all the APs because some of the APs, in particular CR, were not soluble at higher AP concentrations.

APs Decrease the Temperature at Which Cyt *c* Aggregates

An alternative method used in the literature to probe the effects of various solution conditions on protein aggregation is to measure their influence on the temperature at which the protein aggregates during thermal scanning.[11–12,3647–48] We have previously shown that both methods yield similar information, that is, the solution conditions that resulted in faster aggregation of Cyt *c* also exhibited a lower T_m^{Agg}.[36,48] We used a temperature scanning method to monitor the effects of five APs on the T_m^{Agg} of Cyt *c*. For this purpose, we measured the optical density at 695 nm to simultaneously monitor the melting of the least
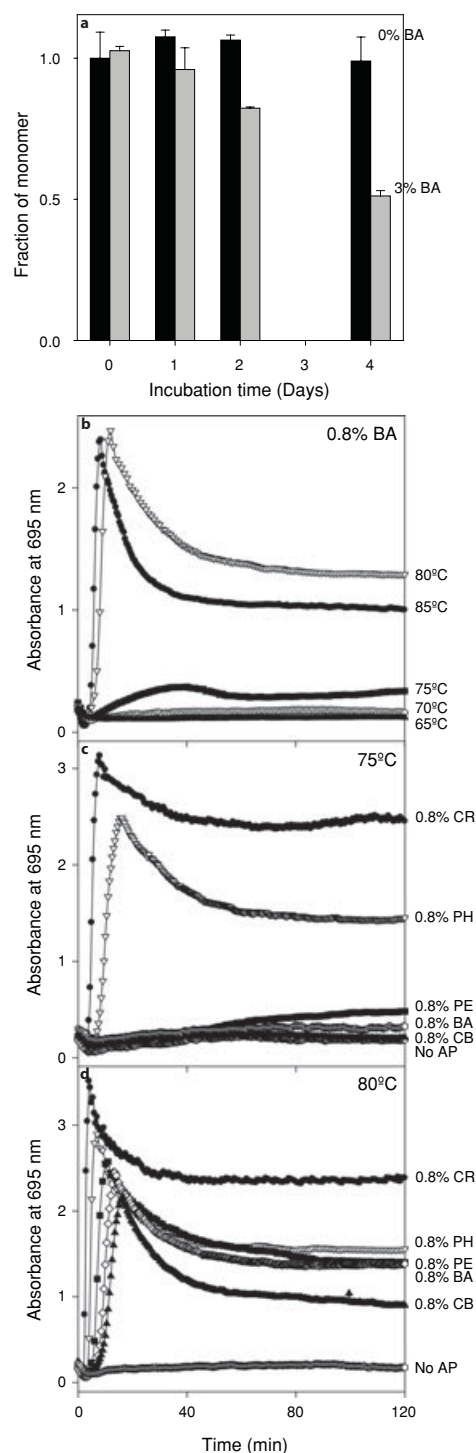

Figure 3. Effect of APs on Cyt *c* aggregation under isothermal conditions. (a) Fraction of soluble monomer remaining in solution after incubation at 37°C with shaking, as determined by size-exclusion chromatography gel filtration. The black and grey bars represent the values without and with 3% (v/v) benzyl alcohol (BA), respectively. (b) Aggregation kinetics at 0.8% (v/v) BA as a function of the solution temperature. (c and d) Aggregation kinetics at 75°C and at 80°C, respectively, at 0.8% (v/v) concentration of the five APs, m-cresol (CR), phenol (PH), phenoxyethanol (PE), benzyl alcohol (BA), and chlorobutanol (CB).
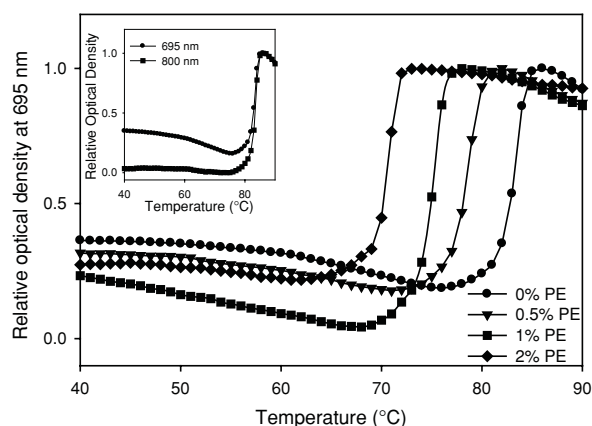
Figure 4. Variation in the optical density at 695 nm as a function of increasing temperature at different concentrations of phenoxyethanol (PE). Inset shows the optical density curve at 695 nm in comparison with that of 800 nm for 0% PE concentration, indicating that the increase in optical density at higher temperatures is due to protein aggregation.

stable structure in Cyt c (Red loop containing Met80 region in Fig. 1) in addition to protein aggregation. In buffer (0% trace in Fig. 4), the optical density initially decreased, indicating unfolding of the local region surrounding Met80. Subsequently, the signal increased until a plateau was reached, which may be because of protein aggregation. We confirmed this by measuring the optical density at 800 nm using the same thermal scanning experiment (Fig. 4, inset). At this wavelength, the protein and the buffer do not absorb, and hence the observed changes in the optical density can be attributed solely to protein aggregation. The increase in optical density at 800 nm as a function of solution temperature exactly matched the latter part of the 695 nm curve (Fig. 4, inset), indicating that the increase in 695 nm signal at higher temperatures is due to aggregation, and not due to the increased absorbance of the Met80 to heme charge transfer band. At much higher temperatures beyond the plateau region, optical density decreased as preformed protein aggregates start settling down to the bottom of the cuvette. We performed this thermal scanning experiment at varying concentrations of PE (Fig. 4) to measure its effect on the T_m^{Agg}. With the addition of PE, the midpoint temperature of aggregation (T_m^{Agg}) decreased, as determined from the 695 nm as well as 800 nm optical density curves. In the absence of PE, the T_m^{Agg} was 83.6°C, whereas the addition of 2% PE decreased the T_m^{Agg} to 69.5°C, indicating that the presence of AP enhanced Cyt c aggregation.

Aggregation Temperature Decreases Linearly with Increasing AP Concentration

Similar to PE, the other four APs decreased the T_m^{Agg} of Cyt c (Fig. 5). A linear correlation was observed be-
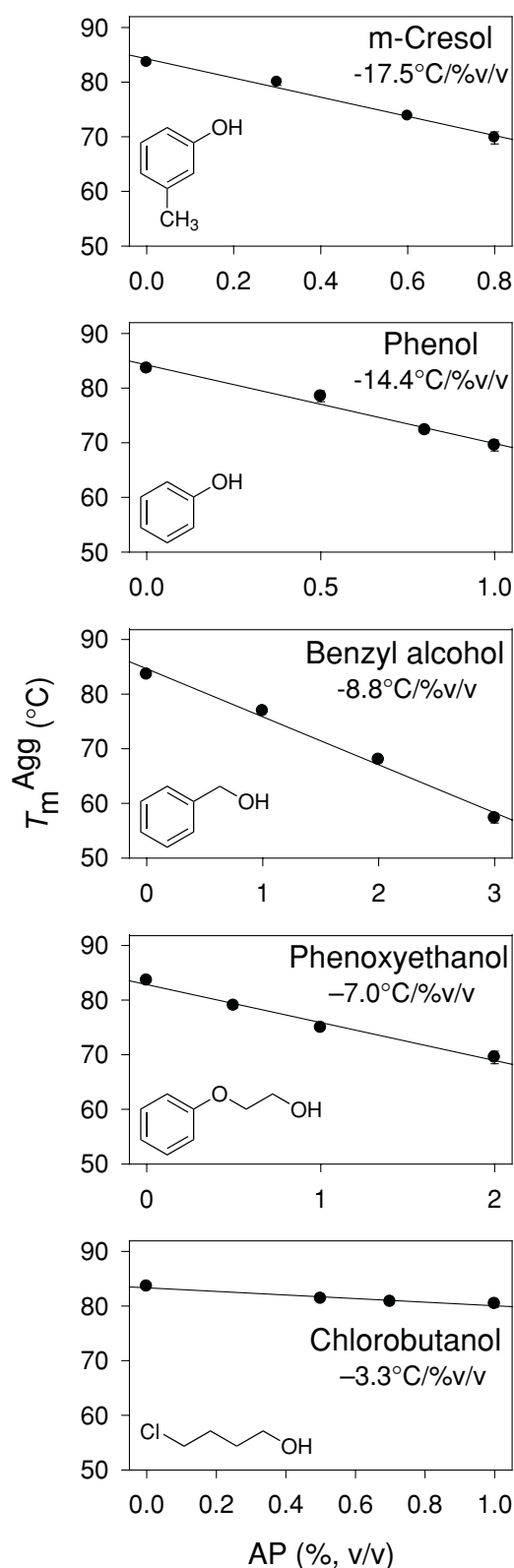

Figure 5. Decrease of the T_m^{Agg} as a function of concentration of the five APs. Individual panels show the slopes of such variation.

tween the concentration of each AP and the T_m^{Agg}. This correlation is significant in that it is a qualitative measure of how effective each preservative is in

inducing the aggregation of Cyt c. By comparing the relative slopes, the five APs induced the aggregation in the order CR > PH > BA > PE > CB. The AP that is most effective in causing protein aggregation is CR. The corresponding slope indicates that for every percent concentration change of CR, the T_m^{Agg} of Cyt c decreases by 17.5°C. In contrast, CB is the least aggregation-causing AP with a slope of 3.3°C/ %v/v. This trend is very similar to that observed from isothermal incubation studies (Fig. 3), except the reversal of the effects of BA and PE.

Unfolding of the Met80 Region Correlates with the T_m^{Agg}

To determine the unifying mechanism underlying AP-induced aggregation, in particular whether the same local protein region acts as an aggregation "hot-spot" for all the APs, we examined the correlation between the unfolding of the local protein region around the residue Met80, which was predicted to be the aggregation "hot-spot",[36] and Cyt c aggregation. As discussed above, the unfolding temperature of the Met80 region (T_m^{695}) was determined from the initial decrease in the absorbance at 695 nm with increase in temperature as the value at which the absorbance is half of the absorbance values of the native and unfolded states (measured independently). A decrease in the absorbance at 695 nm signifies the disruption of the Met80 to heme bond, indicating destabilization of the local structure around Met80 (Fig. 1). This decrease occurred prior to protein aggregation as can be observed by comparing the absorbance traces at 695 and 800 nm (Fig. 4, inset). With the increase in the concentration of the AP, the temperature at which the Met80 region melted decreased (Fig. 4), indicating that the presence of AP destabilized the local structure around Met80. The decrease in T_m^{695} is very similar to that of T_m^{Agg}. We determined the T_m^{695} of all the 16 samples (control with no AP, and three concentrations each of the five APs) from the initial decrease in the optical density at 695 nm (for example, Fig. 4 for PE) and plotted them against T_m^{Agg} (Fig. 6). The relationship between T_m^{695} and T_m^{Agg} was linear ($r^2 = 0.79$), indicating that the destabilization of the Met80 region by the presence of APs may be the critical event that triggers Cyt c aggregation. However, the T_m^{Agg} is higher than T_m^{695} by approximately 10°C–20°C, possibly because of the concentration dependence of protein aggregation. In general, protein unfolding is a unimolecular reaction, whereas protein aggregation is a multimolecular reaction, and hence aggregation is expected to depend on the protein concentration. Consistently, we did not observe Cyt c aggregation when the aggregation experiments were performed at 10 μM protein concentration.[48] With the increase in protein concentration, Cyt c starts aggregating, and
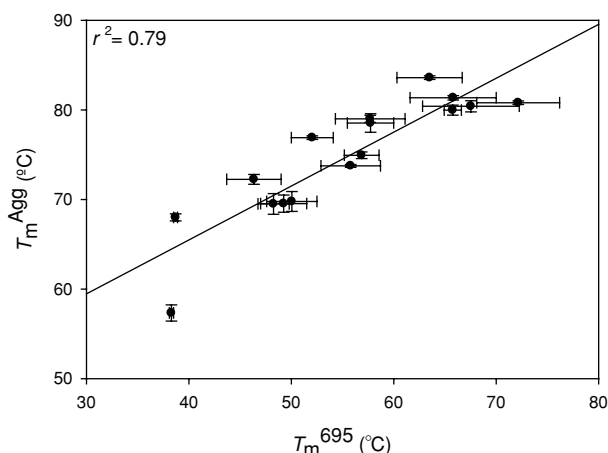

Figure 6. Correlation between the melting temperatures of the Met80 region, T_m^{695}, calculated from the initial decrease in the 695 nm absorbance in thermal scanning (Fig. 4) and the aggregation temperatures, T_m^{Agg}. The plot includes data from 16 sample sets (Cyt c in buffer with no AP, and with each of five APs at three concentrations each).

its T_m^{Agg} shifts to low temperatures, confirming the strong dependence of Cyt c aggregation on its concentration. All the experiments presented in this paper were carried out at a protein concentration of 300 μM.

APs Destabilize the Local Protein Region Around Met80

To further confirm that the presence of APs destabilized the local protein region around Met80, we measured the changes in its stability by monitoring the changes in the 695 nm absorbance with the addition of the denaturant GdmCl (Fig. 7). On the basis of the
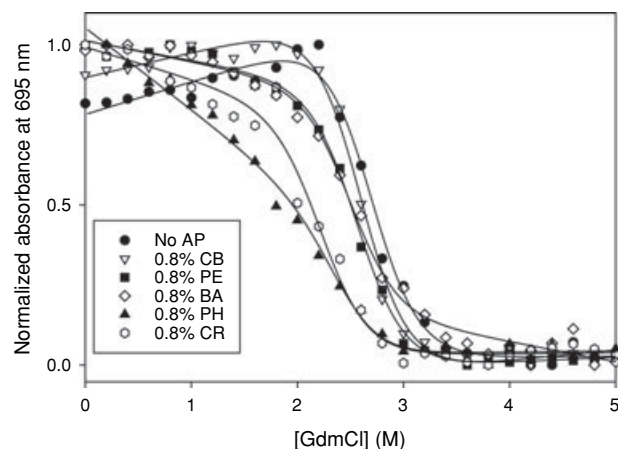

Figure 7. Destabilization of the local protein region around Met80 as monitored by denaturant melts at room temperature. The figure shows the changes in the 695 nm absorbance as a function of GdmCl concentration with different APs. The solid curves show the global fit to a two-state Santoro–Bolen equation.[44–45]

Table 2. Parameters Obtained by Globally Fitting the 695 nm Melting Curves shown in Figure 7, Assuming the Same m Value for all the Curves

AP	ΔG (kcal/mol)	m (kcal/mol/ M[GdmCl])
No AP	7.13 ± 0.39	-2.67 ± 0.15
0.8% CB	6.88 ± 0.38	-2.67 ± 0.15
0.8% PE	6.86 ± 0.38	-2.67 ± 0.15
0.8% BA	6.64 ± 0.38	-2.67 ± 0.15
0.8% PH	6.46 ± 0.40	-2.67 ± 0.15
0.8% CR	5.95 ± 0.39	-2.67 ± 0.15

data in Figure 5, we chose a concentration of 0.8% (v/v) APs for these studies, which is common to all the APs. With the addition of any of the five APs, the decrease in 695 nm shifted to lower denaturant concentration when compared with that in the absence of AP (Fig. 7). These denaturant melts qualitatively indicate that the APs that seriously aggregate Cyt c show a decreased C_m value and a shallower m value, indicating a correlation between partial protein unfolding and aggregation. The decrease in m values may indicate the presence of an intermediate, however, the presence of sloped baselines and the absence of a second, cooperative transition did not result in unique fits to a three-state unfolding model. The sloped baselines in the denaturant melts also resulted in large errors in obtained ΔG values when the individual curves were fit to a two-state model. Therefore, to analyze the effect of APs on protein stability, we assumed that the m value of the partial protein unfolding measured by the decrease in 695 nm absorbance is the same for all the five APs, and all the six melts were globally fit to a two-state model (Fig. 7). The obtained fit parameters are listed in Table 2. The stability decreased in the order CR > PH > BA > PE > CB, which matches the order of the effectiveness of APs in inducing Cyt c aggregation (Fig. 5). To further demonstrate that the APs enhance the unfolding of the Met80 region, we performed amide HX experiments using 2D NMR (Fig. 8). We first monitored the changes in the protein structure using 2D NMR COSY spectra recorded in the absence and presence of the five APs (Fig. 8a). No significant changes were observed in the positions of individual amide cross-peaks, indicating that the APs did not perturb the overall global protein structure. The chemical shifts of main-chain amide and Cα protons of all residues were within 0.1 ppm. We subsequently measured the stability of the Met80 region. For this purpose, we used HX in combination with 2D NMR, which measures the stability of structures around individual amino acids.[49] For an amide proton to be exchanged with the solvent, it needs to be exposed to the solvent, and the exchange rate is proportional to the stability of the structure protecting the amide against exchange. Although individual amide protons exchange through three different

types of unfolding mechanisms,[49] earlier HX experiments on Cyt c indicated that the amides of the two residues Tyr74 and Ile75 exchange with the solvent only upon complete unfolding of the Met80 region.[28] In the absence of APs, these two residues exchange with the rate constants 0.57/h and 0.27/h, respectively. With the addition of APs, the exchange rate of these two residues increased significantly (Fig. 8b). The amide protons exchanged at a much faster rate in the presence of PE (Tyr74: 1.73/h and Ile75: 1.21/h) and BA (Tyr74: 2.60/h and Ile75: 1.19/h), whereas they exchanged within the dead time of the experiment (∼10 min) in the presence of PH and CR. This order in which the APs enhance the amide HX of the Met80 region (Fig. 8b) matches with that of the effectiveness of APs in inducing Cyt c aggregation (Fig. 5).

Stabilizing the Met80 Region Decreases Protein Aggregation

The above results indicate that the Met80 region may be the weakest link whose destabilization triggers Cyt c aggregation. To confirm this and to demonstrate a possible strategy of decreasing protein aggregation, we stabilized the weakest link by reducing the iron in the heme from Fe^{+3} (ferric) to Fe^{+2} (ferrous). Reduction of the heme increases the stability of the bond between Met80 and the heme by 3.2 kcal/mol with no change in the protein structure.[50–51] This is very similar to introducing a site-specific stabilizing mutation in the Met80 region, without the hassle of cloning, expressing, and purifying the mutant protein. The T_m^{Agg} of Cyt c in its reduced (ferrous) state was determined from the change in optical density at 800 nm with increasing solution temperature. No 695 nm absorbance band is seen in the reduced form because of the absence of the charge transfer between Met80 and ferrous iron. Reduction of Cyt c increased the T_m^{Agg} for all five APs and at all AP concentrations. For example, in the presence of 2% PE, oxidized Cyt c has a T_m^{Agg} of 69.5°C, whereas reduced Cyt c has a T_m^{Agg} above 90°C (Fig. 9). In addition, the difference in T_m^{Agg} between the oxidized and reduced forms was nearly identical for different APs (Table 3), indicating that the stabilization of the Met80 region may be the major factor responsible for reducing protein aggregation, consistent with the correlation seen in Figure 6. For most reduced samples, full aggregation curves could not be obtained because of the allowed maximum temperature values in the thermal scanning method, and hence exact T_m^{Agg} values could not be determined.

DISCUSSION

Multidose protein formulations require APs to prevent the accidental growth of microbes during
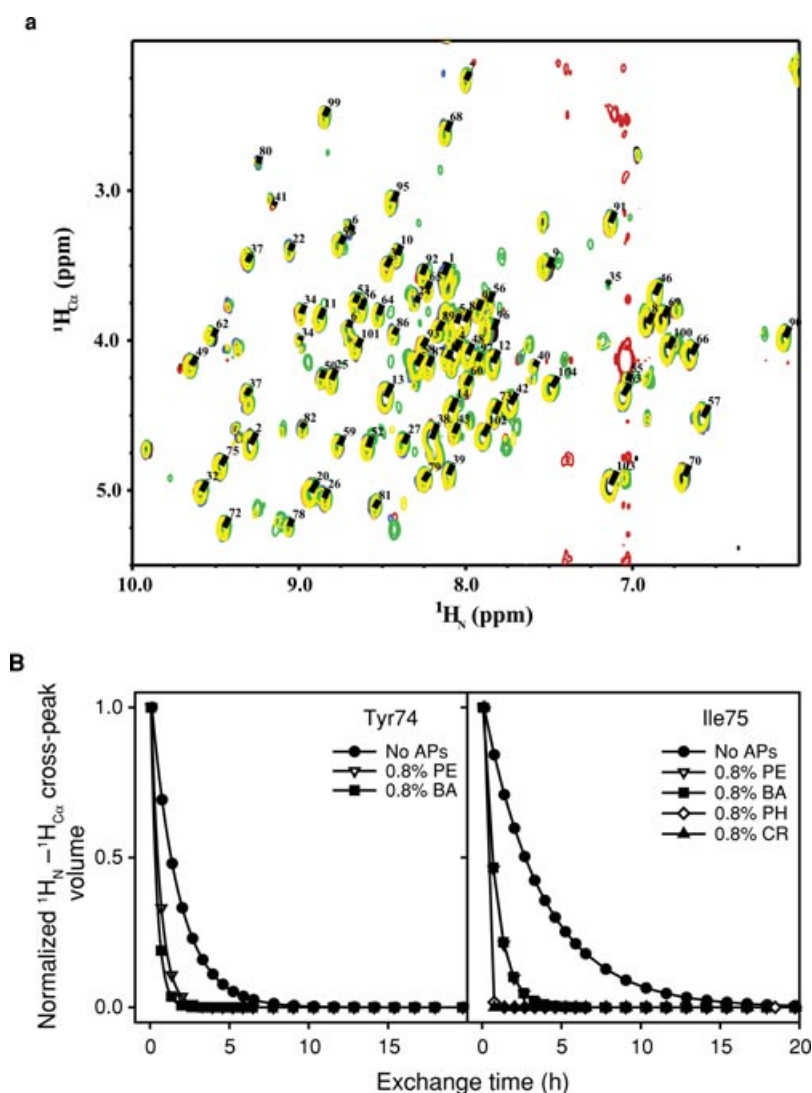
Figure 8. Effect of APs on Cyt *c* solution structure and dynamics. (a) Changes in the 2D NMR COSY fingerprint region with the addition of APs. Black, Red, Blue, Green, and Yellow colors represent the spectra with no AP, 0.8% (v/v) phenoxyethanol (PE), 0.8% (v/v) benzyl alcohol (BA), 0.8% (v/v) phenol (PH), and 0.8% (v/v) m-cresol (CR), respectively. (b and c) Changes in the HX rates of residues Tyr74 and Ile75 with the addition of APs. The exchange of these two "marker" residues represent the partial unfolding of the Met80 region.

repeated use.[3,5] However, APs have been shown to cause protein aggregation,[3,5,9–15] and the underlying physical mechanisms are poorly understood. Here, we used a model protein Cyt *c* to examine the effect of five APs commonly used in liquid protein formulations on protein aggregation (Figs. 3 and 5), and determined the nature of partial protein unfolding that leads to protein aggregation (Fig. 6). We also showed that stabilizing the weakest link, whose unfolding leads to protein aggregation, reduces aggregation (Fig. 9). These results also demonstrate that the same region acts as the aggregation "hot-spot" for all APs, and

Table 3. Comparison of the T_m^{Agg} of Reduced and Oxidized Forms of Cyt *c*

AP	T_m^{Agg} (Oxidized) (°C)	T_m^{Agg} (Reduced) (°C)	ΔT_m^{Agg} (°C)
3% (v/v) BA	57.3	79.9	22.6
2% (v/v) PE	69.5	91.1	21.6
3% (v/v) PE	61.4	84.4	23.0

There is an approximate constant difference between the T_m^{Agg} values indicating that the increase in T_m^{Agg} is predominantly because of the stabilization of the Met80 region due to heme reduction.
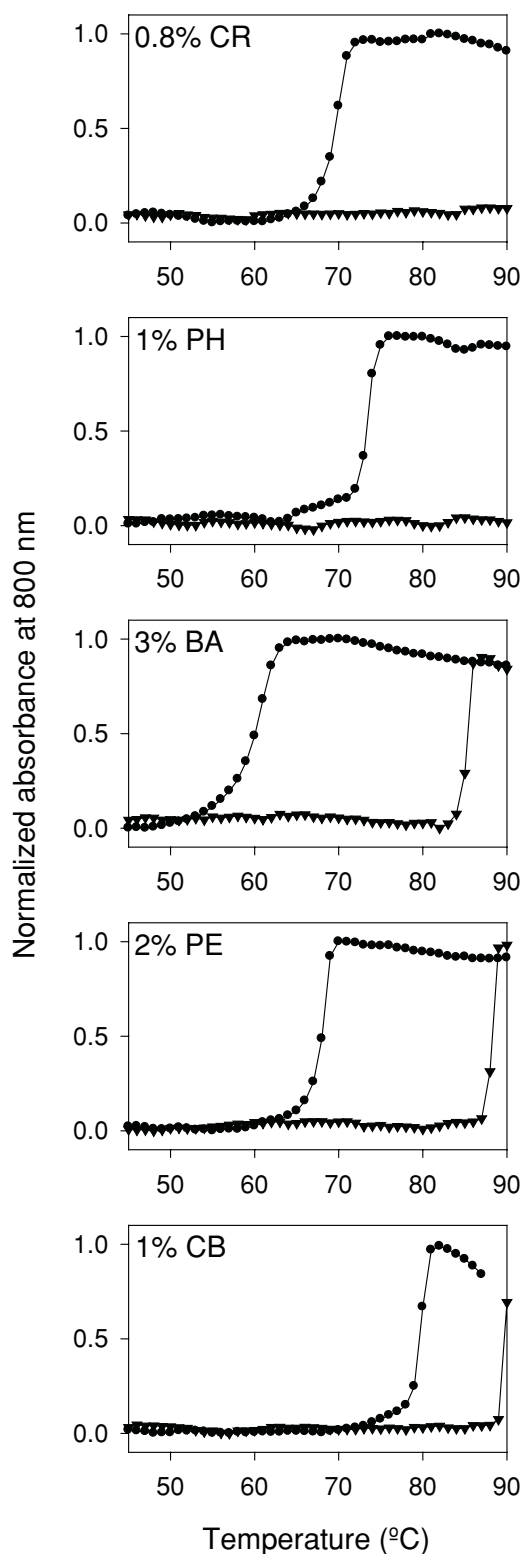
Figure 9. Aggregation of reduced cytochrome *c* (triangles) in comparison with that of the oxidized form (circles). The AP concentrations used were 0.8% (v/v) m-cresol (CR), 1% (v/v) phenol (PH), 3% (v/v) benzyl alcohol (BA), 2% (v/v) phenoxyethanol (PE), and 1% (v/v) chlorobutanol (CB). For all APs, the reduced form aggregated at higher temperatures than the oxidized form.

therefore, any strategies developed to reduce protein aggregation induced by one AP works for all other APs.

The effect of APs on the extent of protein aggregation depends on the nature of the AP. For Cyt *c*, CR is the AP that causes the most aggregation, whereas CB is the AP that causes the least aggregation (Fig. 5). Therefore, if Cyt *c* were a pharmaceutical protein, CB would be the right choice for the AP in its formulation rather than CR. Alternatively, lower concentrations of CR have to be used compared with that of CB, so that CR does not cause protein aggregation. It would be interesting to determine whether the APs follow the same order in terms of inducing aggregation of other proteins, in particular pharmaceutical proteins. In one case where the effect of phenolic compounds, which include three of the APs studied here, on the aggregation of recombinant human growth hormone was examined,[9] the three APs followed a similar trend as that observed here for Cyt *c* (Fig. 5): CR > PH > BA. In another study, CR, PH, and BA caused an antibody to precipitate in formulation, whereas CB showed little to no effect on protein aggregation.[15] The ability of APs to aggregate proteins may depend on the nature of their interactions with proteins, which needs to be determined. Initial studies in this direction indicated that APs do not have strong binding sites on proteins.[11,36] Most of the physical properties that might control protein aggregation, such as hydrophobicity and dielectric constant, have not been characterized for the five APs examined here, and therefore it is not possible at this time to determine which specific physical parameter governs the aggregation reaction.

On the basis of the results presented here, we propose screening of various APs or combinations of APs before selecting the right AP for a protein formulation. The ideal choice for an AP would be the one that causes the least protein aggregation yet possesses the desired antimicrobial effect. At the same time, identifying the weakest link in a protein and measuring the effect of APs on its unfolding might help in reducing protein aggregation, either by introducing site-specific mutations or by modulating solvent properties to stabilize the weakest link. In addition, one needs to ensure that the addition of AP and/or protein modifications do not compromise the function of the therapeutic protein of interest.

Stabilizing the weakest links in pharmaceutical proteins to reduce their aggregation and to improve their shelf-life has been gaining considerable attention in recent years. This is especially important in the case of multidose formulations that need to be stored over long periods of time and preferably at room temperatures in underdeveloped countries. For example, in therapeutic insulin, three amino acid

residues that cause its aggregation have been identified, and mutating these residues decreased aggregation and increased the shelf-life of the formulation at room temperature.[52] In another study, aggregation-prone regions in therapeutic antibodies were identified and were stabilized to reduce aggregation.[53] Our results presented here show that a similar strategy of stabilizing the weakest links in a protein might also decrease its AP-induced aggregation.

Conflict of interest: The authors declare no conflicts of interest.

ACKNOWLEDGMENTS

REFERENCES

1. Trissel LA. 2010. Handbook on injectable drugs. 16th ed. Bethesda, Maryland: American Society of Health-System Pharmacists, Inc.

2. Manning MC, Chou DK, Murphy BM, Payne RW, Katayama DS. 2010. Stability of protein pharmaceuticals: An update. Pharm Res 27:544–575.

3. Meyer BK, Ni A, Hu B, Shi L. 2007. Antimicrobial preservative use in parenteral products: Past and present. J Pharm Sci 96:3155–3167.

4. Cleland JL, Powell MF, Shire SJ. 1993. The development of stable protein formulations—A close look at protein aggregation, deamidation and oxidation. Crit Rev Ther Drug Carrier Syst 10:307–377.

5. Akers MJ, Vasudevan V, Stickelmeyer M. 2002. Formulation development of protein dosage forms. In Development and manufacture of protein pharmaceuticals; Nail SL, Akers MJ, Eds. New York City, New York: Kluwer Academic/Plenum Publishers, pp 47–127.

6. Geier DA, Sykes LK, Geier MR. 2007. A review of thimerosal (Merthiolate) and its ethylmercury breakdown product: Specific historical considerations regarding safety and effectiveness. J Toxicol Environ Health B Crti Rev 10:575–596.

7. Batorova A, Martinowitz U. 2002. Continuous infusion of coagulation factors. Haemophilia 8:170–177.

8. Jorgensen JT, Mortensen HB, Jorgensen JO. 1991. Patient acceptance of Nordiject: A new drug delivery system for growth hormone. DICP: Ann Pharmacother 25:585–588.

9. Maa YF, Hsu CC. 1996. Aggregation of recombinant human growth hormone induced by phenolic compounds. Int J Pharm 140:155–168.

10. Tobler SA, Holmes BW, Cromwell MEM, Fernandez EJ. 2004. Benzyl alcohol-induced destabilization of interferon-γ. J Pharm Sci 39:7161–5061.

11. Roy S, Katayama D, Dong A, Kerwin BA, Randolph TW, carpenter JF. 2006. Temperature dependence of benzyl alcohol-

12. Thirumangalathu R, Krishnan S, Brems DN, Randolph TW, Carpenter JF. 2006. Effects of pH, temperature, and sucrose on benzyl alcohol-induced aggregation of recombinant human granulocyte colony stimulating factor. J Pharm Sci 95:1480–1497.

13. Katakam M, Banga AK. 1997. Use of poloxamer polymers to stabilize recombinant human growth hormone against various processing stresses. Pharm Dev Technol 2:143–149.

14. Remmele Jr. RL, Nightlinger NS, Srinivasan S, Gombotz WR. 1998. Interleukin-1 receptor (IL-1RA) liquid formulation development using differential scanning calorimetry. Pharm Res 15:200–208.

15. Gupta S, Kaisheva E. 2003. Development of a multidose formulation for a humanized monoclonal antibody using experimental design techniques. AAPS Pharm Sci 5:1–9.

16. Ratner RE, Phillips TM, Steiner M. 1990. Persistent cutaneous insulin allergy resulting from high molecular weight insulin aggregates. Diabetes 39:728–733.

17. Thornton CA, Ballow M. 1993. Safety of intravenous immunoglobulin. Arch Neurol 50:135–136.

18. Wright PE, Dyson HJ. 2009. Linking folding and binding. Curr Opin Struct Biol 19:31–38.

19. Hassoun H, Vassiliadis JN, Murray J, Njolstad PR, Rogus JJ, Ballas SK, Schaffer F, Jarolim P, Brabec V, Palek J. 1997. Characterization of the underlying molecular defect in hereditary spherocytosis associated with spectrin deficiency. Blood 90:398–406.

20. Bucciantini M, Giannoni E, Chiti F, Baroni F, Formingli L, Zurdo J, Taddei N, Ramponi G, Dobson CM, Stefani M. 2002. Inherent toxicity of aggregates implies a common mechanism for protein misfolding diseases. Nature 416:507–511.

21. Kaplan JM, Kim SH, North KN, Rennke H, Correia LA, Tong H-Q, Mathis BJ, Rodríguez-Pérez J-C, Allen PG, Beggs AH, Pollak MR. 2000. Mutations in ACTN4, encoding -actinin-4, cause familial focal segmental glomerulosclerosis. Nat Genet 24:251–256.

22. Cheung MS, Chavez LL, Onuchic JN. 2004. The energy landscape for protein folding and possible connections to function. Polymer 45:547–555.

23. Rosenberg AS. 2006. Effects of protein aggregation: An immunologic perspective. AAPS J 8:E501–E507.

24. Robertson SP, Twigg SRF, Sutherland-Smith AJ, Biancalana V, Gorlin RJ, Horn D, Kenwrick SJ, Kim CA, Morava E, Newbury-Ecob R, Ørstavik KH, Quarrell OWJ, Schwartz CE, Shears DJ, Suri M, Kendrick-Jones J, Bacino C, Becker K, Clayton-Smith J, Giovannucci-Uzielli M, Goh D, Grange D, Krajewska-Welasek M, Lacombe D, Morris C, Odent S, Savarirayan R, Stratton R, Superti-Furga A, Verloes A, Vigneron J, Wilcox W, Winter R, Young K, Wilkie AOM. 2003. Localized mutations in the gene encoding the cytoskeletal protein filamin A cause diverse malformations in humans. Nat Genet 33:487–491.

25. Fradkin AH, Carpenter JF, Randolph TW. 2009. Immunogenicity of aggregates of recombinant human growth hormone in mouse models. J Pharm Sci 98:3247–3264.

26. Sauerborn M, Brinks V, Jiskoot W, Schellekens H. 2010. Immunological mechanism underlying the immune response to recombinant human protein therapeutics. Trends Pharmacol Sci 31:53–59.

27. Vazquez-Rey M, Lang DA. 2011. Aggregates in monoclonal antibody manufacturing processes. Biotechnol Bioeng 108:1494–1508.

28. Bai Y, Sosnick TR, Mayne L, Englander SW. 1995. Protein folding intermediates: Native-state hydrogen exchange. Science 269:192–197.

29. Maity H, Maity M, Krishna MMG, Mayne L, Englander SW. 2005. Protein folding: The stepwise assembly of foldon units. Proc Natl Acad Sci USA 102:4741–4746.

30. Krishna MMG, Maity H, Rumbley JN, Lin Y, Englander SW. 2006. Order of steps in the cytochrome *c* folding pathway: Evidence for a sequential stabilization mechanism. J Mol Biol 359:1411–1420.

31. Englander SW, Mayne L, Krishna MMG. 2007. Protein folding and misfolding: Mechanism and Principles. Q Rev Biophysics 40:287–326.

32. Russell BS, Melenkivitz R, Bren KL. 2000. NMR investigation of ferricytochrome c unfolding: Detection of an equilibrium unfolding intermediate and residual structure in the denatured state. Proc Natl Acad Sci USA 97:8312–8317.

33. Maity H, Rumbley JN, Englander SW. 2006. Functional role of a protein foldon—An Ω-loop foldon controls the alkaline transition in ferricytochrome *c*. Proteins 63:349–355.

34. Bandi S, Bowler BE. 2008. Probing the bottom of a folding funnel using conformationally gated electron transfer reactions. J Am Chem Soc 130:7540–7541.

35. Zang C, Stevens JA, Link JJ, Guo L, Wang L, Zhong D. 2009. Ultrafast proteinquake dynamics in cytochrome *c*. J Am Chem Soc 131:2846–2852.

36. Singh SM, Cabello-Villegas J, Hutchings RL, Mallela KMG. 2010. Role of partial protein unfolding in alcohol-induced protein aggregation. Proteins 78:2625–2637.

37. Hirota S, Hattori Y, Nagao S, Taketa M, Komori H, Kamikubo H, Wang Z, Takahashi I, Negi S, Sugiura Y, Kataoka M, Higuchi Y. 2010. Cytochrome *c* polymerization by successive domain swapping at the C-terminal helix. Proc Natl Acad Sci USA 107:12854–12859.

38. Kraulis PJ. 1991. MOLSCRIPT: A program to produce both detailed and schematic plots of protein structures. J Appl Crystallogr 24:945–949.

39. Margoliash E, Frohwirt N. 1959. Spectrum of horse-heart cytochrome *c*. Biochem J 71:570–572.

40. Bowler BE, May K, Zaragoza T, York P, Dong A, Caughey WS. 1993. Destabilizing effects of replacing a surface lysine of cytochrome *c* with aromatic amino acids: Implications for the denatured state. Biochemistry 32:183–190.

41. Creutz C, Sutin N. 1973. Reduction of ferricytochrome c by dithionite ion: Electron transfer by parallel adjacent and remote pathways. Proc Natl Acad Sci USA 6:1701–1703.

42. Sutton SVW, Porter D. 2002. Development of the antimicrobial effectiveness test as USP chapter <51>. PDA J Pharm Sci Techol 65:113–003.

43. Pace CN. 1986. Determination and analysis of urea and guanidine hydrochloride denaturation curves. Methods Enzymol 131:266–280.

44. Santoro MM, Bolen DW. 1988. Unfolding free energy changes determined by the linear extrapolation method. 1. Unfolding of phenylmethanesulfonyl alpha-chymotrypsin using different denaturants. Biochemistry 27:8063–8068.

45. Santoro MM, Bolen DW. 1992. A test of the linear extrapolation of unfolding free energy changes over an extended denaturant concentration range. Biochemistry 31:4901–4907.

46. Feng Y, Roder H, Englander SW, Wand AJ, Stefano DLD. 1989. Proton resonance assignments of horse ferricytochrome c. Biochemistry 28:195–203.

47. Zhang Y, Roy S, Jones LS, Krishnan S, Kerwin BA, Chang BS, Manning MC, Randolph TW, Carpenter JF. 2004. Mechanism for benzyl alcohol-induced aggregation of recombinant human interleukin-1-receptor antagonist in aqueous solution. J Pharm Sci 93:3076–3089.

48. Singh SM, Hutchings RL, Mallela KMG. 2011. Mechanisms of m-cresol-induced protein aggregation studied using a model protein cytochrome c. J Pharm Sci 100:1679–1689.

49. Krishna MMG, Hoang L, Lin Y, Englander SW. 2004. Hydrogen exchange methods to study protein folding. Methods 34:51–64.

50. Xu Y, Mayne L, Englander SW 1998. Evidence for an unfolding and refolding pathway in cytochrome *c*. Nature Struct Biol 5:774–778.

51. Banci L, Bertini I, Huber JG, Spyroulias GA, Turano P. 1999. Solution structure of reduced horse heart cytochrome *c*. J Biol Inorg Chem 4:21–31.

52. Yang Y, Petkova A, Huang K, Xu B, Hua Q-X, Ye I-J, Chu Y-C, Hu S-Q, Phillips NB, Whittaker J, Ismail-Beigi F, Mackin RB, Katsoyannis PG, Tycko R, Weiss MA. 2010. An Achilles' heel in an amyloidogenic protein and its repair. Insulin fibrillation and therapeutic design. J Biol Chem 285:10806–10821.

53. Chennamsetty N, Voynov V, Kayser V, Helk B, Trout BL. 2009. Design of therapeutic proteins with enhanced stability. Proc Natl Acad Sci USA 106:11937–11942.